Supplementary Information

Crystal Phase Effect upon O_2 Activation on Gold Surfaces through Intrinsic Strain

Lixiang Zhong and Shuzhou Li*

School of Materials Science and Engineering, Nanyang Technological University, Singapore 639798, Singapore

**E-mail: lisz@ntu.edu.sg*

1. Computational Methods

Spin-unrestricted calculations were performed using density functional theory as implemented in the Vienna *ab initio* simulation package (VASP).[1-2] The ion-electron interactions are treated with the projected augmented wave pseudopotentials,[3] and the plane-wave basis set was cut off at 400 eV. Generalized gradient approximation with the Perdew-Burke-Ernzerhof functional was used to determine the exchange-correlation energy.[4] The slab model was adopted to mimic the metal surfaces and the separation between two slabs was larger than 15 Å to eliminate spurious interactions. A six-layer slab with 3×3 surface unit cell was adopted when simulating the oxygen adsorption and O_2 dissociation on the Au(111) surface with different crystal phases, and a 7×7×1 *k*-point mesh was sampled by the Monkhorst-Pack scheme.[5] The 1×1 (111) unit cell was used when studying the layer number effect, and the corresponding *k*-point mesh was increased to 21×21×1. All structures were optimized by the conjugate gradient method until the residual force on each unfixed atom was less than 0.01 eV/Å, and only the lower half of the slab was fixed. The climbing image nudged elastic band method was used to find the transition states and calculate the corresponding energy barriers.[6] The DFT-D3 method with Becke-Jonson damping was adopted to include van der Waals interactions and was only applied in the simulations of O_2 dissocications,[7-8] which involve the adsorption of O_2 on gold surfaces. In addition, the structure models were visualized in the VESTA software.[9]

2. Structural Parameters

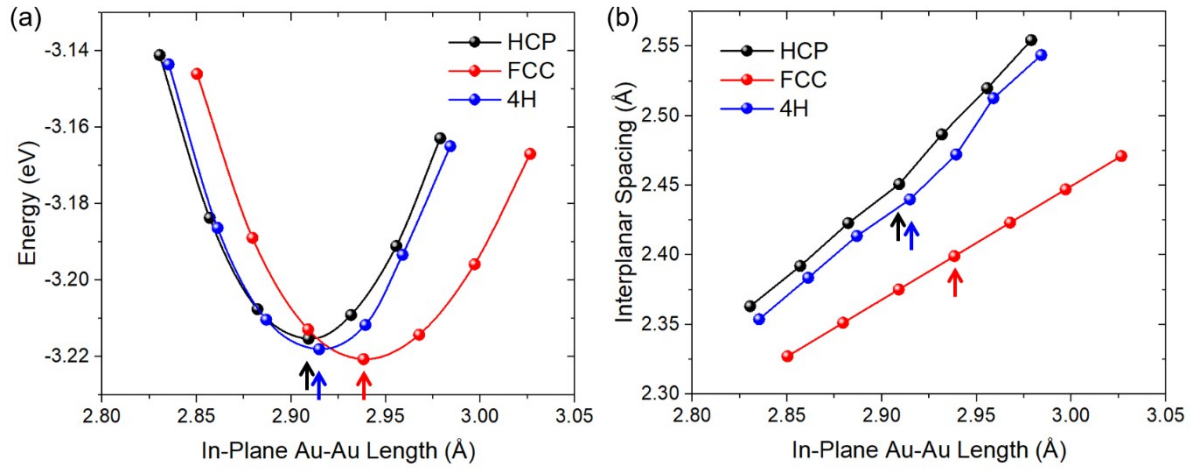

Figure S1. (a) Potential energy per atom of gold with different crystal phases under isotropic strain as a function of in-plane Au-Au length. (b) Nearly linear relationship between interplanar spacing and in-plane Au-Au length under isotropic strain.

Table S1. The structural parameters of HCP, FCC, and 4H bulk gold.

	HCP	**FCC**	**4H**
Stacking sequence	… AB …	… ABC …	… ABCB …
Interplanar spacing (Å)	2.451 2.451[ref 10]	2.399 2.409[ref 10]	2.440
In-plane Au-Au length (Å)	2.909 2.927[ref 10]	2.938 2.951[ref 10]	2.915

Table S2. The structural parameters of HCP, FCC, and 4H free-standing 6-layer gold nanosheets.

	HCP	**FCC**	**4H**
Stacking sequence	… AB …	… ABC …	… ABCB …
Interplanar spacing (Å)	2.536	2.521	2.520
In-plane Au-Au length (Å)	2.871	2.873	2.874

3. Dissociation of O_2

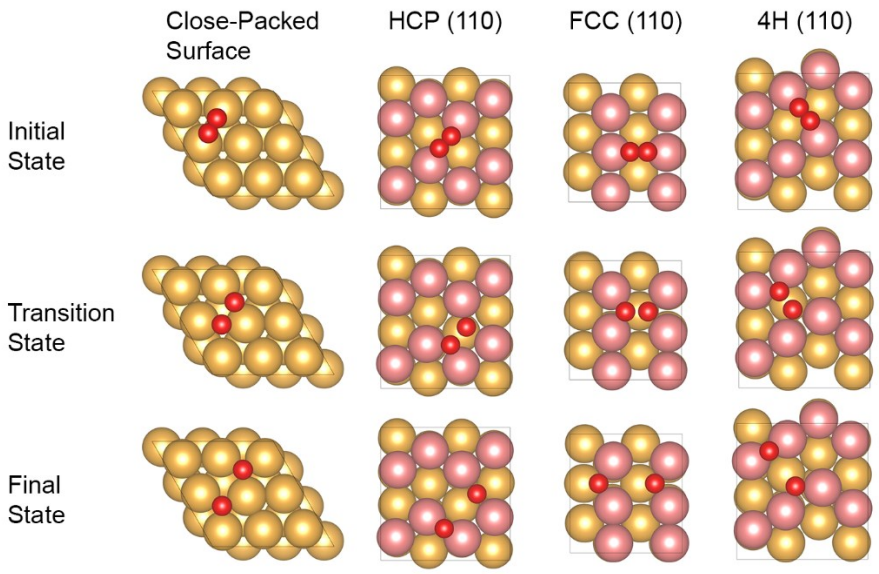

Figure S2. Dissociation processes of O_2 on close-packed and (110) gold surfaces with different crystal phases.

4. Layer Number Effect

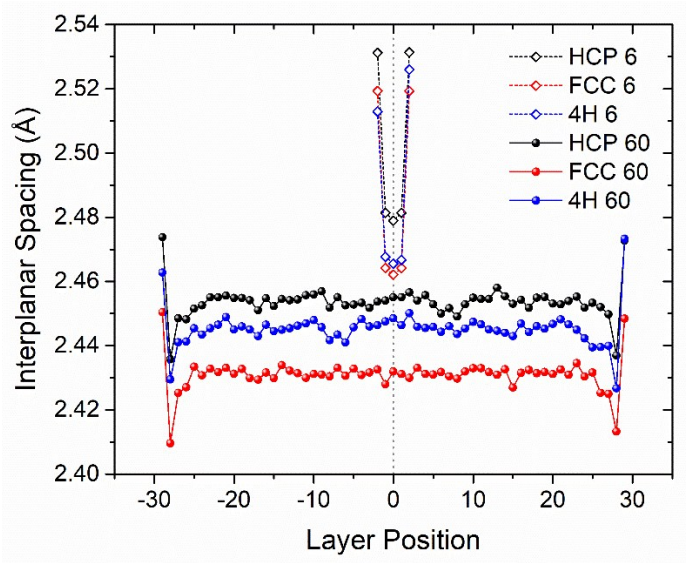

Figure S3. Distribution of interplanar spacing in 6-layer and 60-layer gold nanosheets with different crystal phases.

Reference

(1) Kresse, G.; Furthmüller, J. Efficiency of Ab-Initio Total Energy Calculations for Metals and Semiconductors Using a Plane-Wave Basis Set. *Comput. Mater. Sci.* **1996**, *6*, 15-50.

(2) Kresse, G.; Furthmüller, J. Efficient Iterative Schemes for Ab Initio Total-Energy Calculations Using a Plane-Wave Basis Set. *Phys. Rev. B* **1996**, *54*, 11169-11186.

(3) Blochl, P. E. Projector Augmented-Wave Method. *Phys. Rev. B* **1994**, *50*, 17953-17979.

(4) Perdew, J. P.; Burke, K.; Ernzerhof, M. Generalized Gradient Approximation Made Simple. *Phys. Rev. Lett.* **1996**, *77*, 3865-3868.

(5) Methfessel, M.; Paxton, A. T. High-Precision Sampling for Brillouin-Zone Integration in Metals. *Phys. Rev. B* **1989**, *40*, 3616-3621.

(6) Henkelman, G.; Uberuaga, B. P.; Jonsson, H. A Climbing Image Nudged Elastic Band Method for Finding Saddle Points and Minimum Energy Paths. *J. Chem. Phys.* **2000**, *113*, 9901-9904.

(7) Grimme, S.; Antony, J.; Ehrlich, S.; Krieg, H. A Consistent and Accurate Ab Initio Parametrization of Density Functional Dispersion Correction (DFT-D) for the 94 Elements H-Pu. *J. Chem. Phys.* **2010**, *132*, 154104.

(8) Grimme, S.; Ehrlich, S.; Goerigk, L. Effect of the Damping Function in Dispersion Corrected Density Functional Theory. *J. Comput. Chem.* **2011**, *32*, 1456-1465.

(9) Momma, K.; Izumi, F. VESTA 3 for Three-Dimensional Visualization of Crystal, Volumetric and Morphology Data. *J. Appl. Crystallogr.* **2011**, *44*, 1272-1276.

(10) Wang, Y.; Curtarolo, S.; Jiang, C.; Arroyave, R.; Wang, T.; Ceder, G.; Chen, L. Q.; Liu, Z. K. Ab Initio Lattice Stability in Comparison with Calphad Lattice Stability. *Calphad* **2004**, *28*, 79-90.